fractal and fractional

MDPI

Article

On Fuzzy and Crisp Solutions of a Novel Fractional Pandemic Model

Kalpana Umapathy [1], Balaganesan Palanivelu [1], Víctor Leiva [2,*], Prasantha Bharathi Dhandapani [3,*] and Cecilia Castro [4]

[1] Department of Mathematics, AMET Deemed to be University, Chennai 603112, Tamil Nadu, India; kalpana21@ametuniv.ac.in (K.U.); balaganesan.p@ametuniv.ac.in (B.P.)
[2] School of Industrial Engineering, Pontificia Universidad Católica de Valparaíso, Valparaíso 2362807, Chile
[3] Department of Mathematics, Sri Eshwar College of Engineering, Coimbatore 641202, Tamil Nadu, India
[4] Centre of Mathematics, Universidade do Minho, 4710-057 Braga, Portugal; cecilia@math.uminho.pt
* Correspondence: victor.leiva@pucv.cl or victorleivasanchez@gmail.com (V.L.); prasanthabharathi.d@sece.ac.in or d.prasanthabharathi@gmail.com (P.B.D.)

Abstract: Understanding disease dynamics is crucial for accurately predicting and effectively managing epidemic outbreaks. Mathematical modeling serves as an essential tool in such understanding. This study introduces an advanced susceptible, infected, recovered, and dead (SIRD) model that uniquely considers the evolution of the death parameter, alongside the susceptibility and infection states. This model accommodates the varying environmental factors influencing disease susceptibility. Moreover, our SIRD model introduces fractional changes in death cases, which adds a novel dimension to the traditional counts of susceptible and infected individuals. Given the model's complexity, we employ the Laplace-Adomian decomposition method. The method allows us to explore various scenarios, including non-fuzzy non-fractional, non-fuzzy fractional, and fuzzy fractional cases. Our methodology enables us to determine the model's equilibrium positions, compute the basic reproduction number, confirm stability, and provide computational simulations. Our study offers insightful understanding into the dynamics of pandemic diseases and underscores the critical role that mathematical modeling plays in devising effective public health strategies. The ultimate goal is to improve disease management through precise predictions of disease behavior and spread.

Keywords: decomposition; epidemic models; fractional changes; Laplace-Adomian; stability

Citation: Umapathy, K.; Palanivelu, B.; Leiva, V.; Dhandapani, P.B.; Castro, C. On Fuzzy and Crisp Solutions of a Novel Fractional Pandemic Model. *Fractal Fract.* **2023**, *7*, 528. https://doi.org/10.3390/fractalfract7070528

Academic Editor: Gani Stamov

Received: 27 May 2023
Revised: 20 June 2023
Accepted: 25 June 2023
Published: 4 July 2023

1. Introduction and Background

Epidemic modeling, a crucial subfield of mathematical biology [1], has provided invaluable insights into comprehending and forecasting disease dynamics [2–6]. The well-being of individuals is frequently influenced by diverse environmental factors, such as air pollution, contaminated water, and climate fluctuations, rendering us susceptible to a broad range of diseases [7]. Within this spectrum, infectious diseases transmitted through various means pose a substantial global health challenge [8].

When these infectious diseases affect a localized population, they are considered epidemics. However, when such diseases cross geographical boundaries and affect individuals on a global scale, they evolve into pandemics. Effective management of these diseases heavily depends on our ability to predict their behavior and spread, a task often accomplished through mathematical models [9–11].

In the field of fuzzy mathematics [12,13], the introduction of fuzzy sets marked a significant advancement [14], and the progress was furthered with the proposal of fuzzy differential equations [15]. Additionally, an extension of the Newton method for a system of nonlinear equations was introduced by using a modified version of the Laplace-Adomian decomposition method (LADM) [16–19], a method that has been applied in the analysis of nonlinear systems related to diseases.

In light of the emergence and impact of recent pandemics, considerable research has been conducted to improve our understanding of the disease [20]. Novel dynamic aspects of the susceptible, exposed, infected, and recovered (SEIR) epidemic model [21] have been presented with applications in the understanding of diseases such as COVID-19 [5]. More recent studies have delved into the dynamics of a susceptible, infectious, recovered, and vaccinated (SIRV) model [22], employing the LADM in conjunction with a vaccination strategy [23]. Numerical solutions for a differential system considering a pure hybrid fuzzy neutral delay theory were also provided, offering new insights into disease modeling [24]. A fractional influenza model was presented in [25]. A stochastic model for the COVID-19 outbreak was stated in [26]. The dynamics of the COVID-19 pandemic in India under lockdown was introduced in [27]. In [28], modeling of the COVID-19 dynamics with fractional derivatives was carried out [29]. A fractional model and optimal control of tumor surveillance with a non-singular derivative operator was presented in [30]. In [31], an estimator for discrete-time SEIR epidemic models was proposed.

Now, new approaches to disease modeling are being considered, such as the use of a fractal-fractional model that addresses the psychological effects of COVID-19 [7]. Similarly, a comprehensive model for the hepatitis B virus infection that includes vaccination and hospitalization through a fractional framework has been developed, expanding our understanding of disease dynamics [32]. Furthermore, a new regression model for fractiles has been proposed, which proves particularly beneficial in handling covariate-related response variables that frequently arise in disease data.

Machine learning techniques are also being employed for tasks such as classifying COVID-19 based on amino acid encoding [33] and predicting COVID-19 trends [34]. Studies have also utilized mathematical modeling to evaluate the impact of COVID-19 on the economy [35] and predict cryptocurrency returns based on gold prices during the pandemic [36]. Statistical analyses for the epidemiological surveillance of COVID-19 have also been performed [37], along with the development of data-driven tools for assessing and combating COVID-19 outbreaks [38]. Principal component analysis has been employed to study infected cases and deaths due to COVID-19 in South American countries [39]. Survival models employing Weibull regression and machine learning have been applied to biomedical data related to cardiac surgery [40], while autoregressive moving average time series models have been stated in [35] for financial applications under the COVID-19 pandemic [35]. All of these advancements in epidemic modeling demonstrate its ongoing evolution, with researchers increasingly turning towards complex mathematical methods and computational tools to better understand and predict disease behavior. Therefore, the objective of the present study is to develop a new epidemic model based on susceptible, infected, recovered, and death cases (SIRD).

This article is divided into four sections. In Section 1, we provided an overview of the research field and outline the proposed SIRD model. Section 2 clarifies essential concepts and introduces the analytical strategies. In Section 3, the findings from applying the model are presented and discussed, which is further divided into the analytical solution to the problem and the fuzzy-valued solutions. Finally, Section 4 concludes the main findings of the study, along with implications and directions for future research.

2. Methodology

In this section, we state a detailed explanation of the methodology used in our study.

2.1. SIRD Epidemic Model

Consider the fuzzy fractional model under an Atangana–Baleanu Caputo (ABC) derivative, ${}^{ABC}\Delta^{\alpha} f(t)$ namely. This model is closed as we assume no new birth or death will occur. The model is based on the following: an unknown disease spreads in a place where there are a few susceptible, infected, and recovered individuals, and a few have died out of the overall population. We assume that at the stage of observation, it is noted that a few people died due to the severity of the disease, lack of immunity, or lack of medication.

We also assert that no new individuals were further deceased or are expected to be susceptible. This model aims to improve the susceptible, infectious, and recovered (SIR) epidemic model [41,42]. The classical epidemic models do not account for changes in susceptible, infected, and deceased cases (SID). In any common flu or severe disease, it is natural that some people recover, some die, and the recovered people may become infected again. Recovered individuals are also part of the susceptible group. Both recovered and deceased individuals are free from infection, but the recovered individuals may become infected again or even die naturally, whereas deceased individuals would not become infected, susceptible, or recovered. Thus, the SIRD model is an extended version of the traditional SIR model, including an additional D compartment for those who have succumbed to the disease, which allows one to gain more accurate and comprehensive insights into the progression and impact of the disease in the population [43,44]. Furthermore, the SIRD model provides the ability to differentiate the rates of mortality from the recovery rates, which can provide critical information in evaluating the severity and managing the outbreak. The model given in (1) enhances the SIRD model further by integrating it with a fuzzy fractional-order system, providing a more flexible and sophisticated tool to handle the inherent uncertainty and complexity associated with real-world epidemic scenarios [45]. The model accounts for uncertain parameters in the transmission dynamics, which better characterizes the practical uncertainties such as heterogeneity in population, the stochastic nature of human behaviors, and unpredictability in disease progression. This model is formulated as

$$\begin{array}{rcl} \Delta S(t) & = & -\beta S(t)I(t) \\ \Delta I(t) & = & \beta S(t)I(t) - (\delta + \psi)I(t) \\ \Delta R(t) & = & (\delta - \psi)I(t) - \psi R(t) \\ \Delta D(t) & = & (\psi - \delta)I(t) - \psi D(t), \end{array} \tag{1}$$

with $\Delta = \mathrm{d}/\mathrm{d}t$, a time derivative representing the rate of change in the population of susceptible, infected, recovered, and dead individuals.

We develop a new SIRD epidemic model for which we require parameters (rates) β, δ, and ψ according to Figure 1, where β is the transition rate from susceptible (S) to infected (I), δ is the rate from infected (I) to recovered (R), and ψ is the rate from infected (I) to deceased (D). These rates are crucial in understanding the spread of a disease in a population.

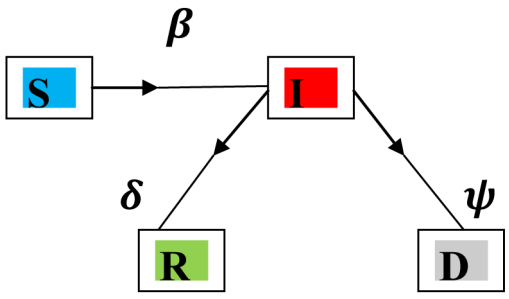

Figure 1. Model formulation and compartment transition rates.

2.2. Preliminary Concepts and Definitions

Next, we present some known results of fractional differential equations in terms of fuzzy numbers [46]. We propose a modification by using the ABC derivative instead of the integer derivative given in the model stated in (2). The motivation behind this modification is rooted in the characteristics of fractal-fractional calculus.

Fractional calculus allows for derivatives and integrals of non-integer orders, providing a tool to model real-world phenomena more accurately compared to classical integer-order calculus. The transition to fractional calculus in the context of epidemiological models provides a higher degree of freedom, capturing the complexity and anomalous dynamics inherent in the spreading process of diseases.

Furthermore, the ABC derivative represents a specific type of fractional derivative, incorporating the concept of fractal dimensions. Indeed, fractal dimensions describe situations where data are between two integers, offering a sophisticated representation of real-world systems that exhibit non-integer dimensions due to their complex, irregular, and fragmented structure. The ABC derivative, by integrating the fractal dimension with the fractional order, helps in capturing the intricacies of disease propagation more realistically.

As a result, the system of differential equations stated in (1) can be rewritten as a fractional system of differential equations (FSDE) in terms of ABC derivatives, as presented in (2). This FSDE encapsulates the complex and non-linear nature of the SIRD model, providing a more realistic tool to understand and predict the course of epidemics. Choice of the ABC derivative over the integer derivative stems from its ability to provide more realistic results by considering the fractal nature of real-world phenomena, for example, the spread of diseases in populations.

Definition 1 ([8,47])**.** The ABC fractional derivative is defined for a function f over the interval $[0, t]$ as

$$^{\mathrm{ABC}}\Delta^{\alpha}_{[0,t]}f(t) = \frac{F(\alpha)}{(1-\alpha)}\int_0^t f'(\mu)\mathcal{E}_{\alpha}\left(-\frac{\alpha(t-\mu)^{\alpha}}{(1-\alpha)}\right)\mathrm{d}\mu,$$

where $0 < \alpha \leq 1$ is the fractional order and the Mittag-Leffler function of order α is given by

$$\mathcal{E}_{\alpha}(z) = \sum_{k=0}^{+\infty}\frac{z^k}{\Gamma(k\alpha+1)}.$$

As in the Caputo–Fabrizio case [47], $F(\alpha) = (1-\alpha)/\Gamma(1-\alpha)$ is a normalization function that satisfies $F(0) = F(1) = 1$.

Definition 2 ([8])**.** The Laplace transform of the ABC derivative is presented as

$$\mathcal{L}\{^{\mathrm{ABC}}\Delta^{\alpha}_{[0,t]}f(t)\}(s) = \frac{F(\alpha)}{(1-\alpha)}\left(\frac{s^{\alpha}\mathcal{L}\{f(t)\}(s) - s^{\alpha-1}}{s^{\alpha}+\alpha/(1-\alpha)}\right),$$

where $0 < \alpha \leq 1$.

Definition 3 ([8])**.** The Atangana–Baleneanu integral of a function $f(t)$ of order $\alpha > 0$ is established as

$$^{\mathrm{ABC}}J^{\alpha}_{[0,t]}f(t) = \frac{(1-\alpha)}{F(\alpha)}f(t) + \frac{\alpha}{F(\alpha)\Gamma(\alpha)}\int_0^t f(\mu)(t-\mu)^{\alpha-1}\mathrm{d}\mu.$$

The integral combines the function $f(t)$, the normalization function $F(\alpha)$, and the usual gamma function. It converges to a classical integral as α approaches 1.

Next, we present the FSDE consisting of four equations describing the dynamics of a SIRD model as

$$\begin{aligned}
^{\mathrm{ABC}}\Delta^{\alpha_1}S(t) &= -\beta S(t)I(t)\\
^{\mathrm{ABC}}\Delta^{\alpha_2}I(t) &= \beta S(t)I(t) - (\delta+\psi)I(t)\\
^{\mathrm{ABC}}\Delta^{\alpha_3}R(t) &= (\delta-\psi)I(t) - \psi R(t)\\
^{\mathrm{ABC}}\Delta^{\alpha_4}D(t) &= (\psi-\delta)I(t) - \psi D(t).
\end{aligned} \tag{2}$$

In the fuzzy fractional order system of differential equations, the same four expressions presented in (2) are modified by introducing fuzzy numbers $(0.75 + 0.25r, 1.125 - 0.125r)$, with $r \in [0, 1]$, to state uncertain parameters and then we have

$$\begin{array}{rcl} {}^{ABC}\Delta^{\alpha_1}\widetilde{S}(t) & = & (0.75 + 0.25r, 1.125 - 0.125r)(-\beta S(t)I(t)) \\ {}^{ABC}\Delta^{\alpha_2}\widetilde{I}(t) & = & (0.75 + 0.25r, 1.125 - 0.125r)(\beta S(t)I(t) - (\delta + \psi)I(t)) \\ {}^{ABC}\Delta^{\alpha_3}\widetilde{R}(t) & = & (0.75 + 0.25r, 1.125 - 0.125r)(\delta - \psi)I(t) - \psi R(t) \\ {}^{ABC}\Delta^{\alpha_4}\widetilde{D}(t) & = & (0.75 + 0.25r, 1.125 - 0.125r)(\psi - \delta)I(t) - \psi D(t). \end{array} \tag{3}$$

In the particular utilization of the fuzzy fractional order system of differential equations, a fuzzification process is employed. In this process, any given function, $f(t)$ say, is altered into its fuzzy equivalent according to the universal rule given by

$$\tilde{f}(t) = (0.75 + 0.25r, 1.125 - 0.125r)f(t),$$

with $r \in [0, 1]$ acting as the common guideline for the fuzzification of functions or parameters. In this context, $r \in [0, 1]$ symbolizes the degree of fuzziness, where 0 corresponds to certainty while 1 represents the maximum level of uncertainty.

In the ensuing discourse and in various figures throughout this document, we represent these fuzzy functions simply as $S(t)$, $I(t)$, $R(t)$, and $D(t)$ for the sake of brevity and clarity. Nonetheless, it is crucial to remember that these representations stand for their fuzzy counterparts with a fuzziness degree in the range $r \in [0, 1]$.

Moving on to initial conditions, it is assumed that the total population size, denoted by N, remains constant. This total is derived from the sum of initial populations of susceptible, infected, recovered, and deceased individuals, mathematically expressed as $S(0) + I(0) + R(0) + D(0) = N$. The specific initial population values are given as $S(0) = S_0 = m_1 = 350$, $I(0) = I_0 = m_2 = 400$, $R(0) = R_0 = m_3 = 400$, and $D(0) = D_0 = m_4 = 350$. Hence, we introduce the parameters β, δ, and ψ, each representing a distinct rate associated with the disease dynamics, where β denotes the rate at which the susceptible individuals become infected, given as 0.0007; δ characterizes the rate at which the infected individuals recover, given as 0.09; and ψ signifies the rate at which the infected individuals succumb to the disease, given as 0.08.

2.3. Equilibrium and Stability Snalyses

We examine the equilibrium state [48] of the epidemic model and its stability [49,50]. The basic reproduction number, denoted as B_0, is particularly important for understanding the potential of an outbreak. Note that B_0 represents the number of secondary infections produced by a single infected individual throughout the epidemic period. This number is calculated from the rate of change in the population of infected individuals at the initial time point $t = 0$. When

$${}^{ABC}\Delta^{\alpha_2}I(t_0) = 0,$$

we have

$$\beta S(t_0)I(t_0) - (\delta + \psi)I(t_0) = 0,$$

which simplifies to

$$\beta S_0 I_0 - (\delta + \psi)I_0 = 0,$$

and it further reduces to

$$I_0(\beta S_0 - (\delta + \psi)) = 0.$$

This last expression gives

$$\beta S_0 = \delta + \psi,$$

which yields

$$S_0 = \frac{\delta + \psi}{\beta}.$$

Then, the basic reproduction number is given by

$$B_0 = \frac{S_0\beta}{\delta+\gamma},$$

where $(\psi+\delta)/\beta = S_c$. If the initial number of susceptible individuals, S_0 say, is less than the critical threshold, Sc, the disease will not persist in the population. In addition, if $S_0 > S_c$, the disease is expected to resurge, leading to an epidemic. In our model, the estimated B_0 is approximately 1.44, indicating a likelihood of subsequent waves of infection, especially when $S_0 > S_c$. Thus, if $S_0 = 350$ and $S_c = 242.86$ (approximately), the disease is expected to resurge because S_0 is greater than S_c. These conditions suggest that our model represents a pandemic growth scenario, where the disease continues to spread and recur within the population.

Now, we analyze the equilibrium points of the FSDE presented in (2) under the conditions stated as

$$\text{ABC}\Delta^{\alpha_1}S(t) = 0, \quad {}^{\text{ABC}}\Delta^{\alpha_2}I(t) = 0, \quad {}^{\text{ABC}}\Delta^{\alpha_3}R(t) = 0, \quad {}^{\text{ABC}}\Delta^{\alpha_4}D(t) = 0.$$

Under these conditions, the system has a disease-free equilibrium point given by $\text{DFEP} = (0,0,0,0)$. It also possesses disease-dependent equilibrium points (DDEP) formulated as

$$\text{DDEP} = \left(\frac{\delta+\psi}{\beta}, I(t_0), \frac{(\delta-\psi)I(t_0)}{\psi}, \frac{(\psi-\delta)I(t_0)}{\psi}\right) = (242.857, 400, 50, -50).$$

To determine whether the model is asymptotically stable, we check if all the eigenvalues of the linearized form of the FFDE are less than zero. Let us begin by linearizing the FFDE given by (2) in the form of the Jacobian matrix expressed as

$$\mathcal{J} = \begin{pmatrix} -\beta I(t) & -\beta S(t) & 0 & 0 \\ \beta I(t) & \beta S(t) - (\delta+\psi) & 0 & 0 \\ 0 & \delta-\psi & -\psi & 0 \\ 0 & \psi-\delta & 0 & -\psi \end{pmatrix}.$$

Thus, the characteristic polynomial of $\mathcal{J}$ is found to be

$$0.00031 + 0.00893\lambda + 0.08680\lambda^2 + 0.36500\lambda^3 + \lambda^4.$$

Then, the corresponding eigenvalues are $-0.1025 + 0.1926\,\mathrm{i}$, $-0.1025 - 0.1926\,\mathrm{i}$, -0.0800, and -0.0800, respectively, where i is the complex number. Note that all the eigenvalues have negative real parts. As shown in Figure 2, the complex plane portrait illustrates that the negative real parts of the eigenvalues lie within the second and third quadrants, that is, the left half of the complex plane. Therefore, we conclude that the system we have considered is asymptotically stable, and the model exhibits stable dynamics around the equilibrium points.

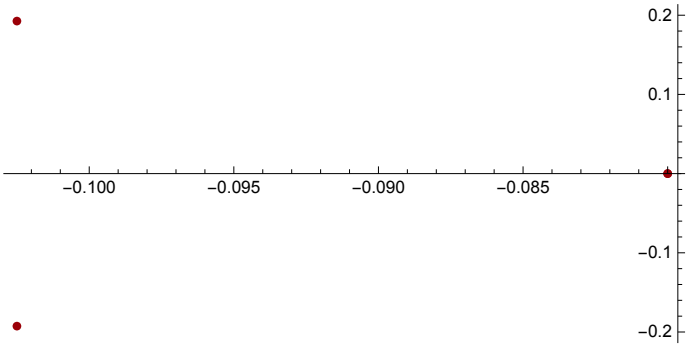

Figure 2. Complex plane plot.

2.4. Positive Boundedness of Solutions

Next, we conduct an analysis of the positivity and boundedness of the solutions, which are crucial for any epidemic model. Positivity ensures that the solutions, representing the population of each compartment, remain non-negative over time, mirroring the biological reality of non-negative populations. Boundedness guarantees that the solutions do not increase indefinitely but rather remain within a certain range, considering the finite size of the population. It become a mandatory aspect when dealing with the real-world situations to establish that the results are bounded positively. Thus, we are presenting here the analysis of positiveness of the solutions. From the formulations given in (1) and (2), we obtain the solutions of $S(t)$, $I(t)$, $R(t)$, and $D(t)$ expressed as

$$\begin{aligned}
S(t) &= S(t_0) + \mathrm{e}^{-\beta \int_{t_0}^{t} I(k)\mathrm{d}k}, \quad 0 < S(t) < +\infty, \\
I(t) &= I(t_0) + \mathrm{e}^{\int_{t_0}^{t} (\beta S(k) - (\delta+\psi))\mathrm{d}k}, \quad 0 < I(t) < +\infty, \\
R(t) &= \mathrm{e}^{-r(t-t_0)}(R(t_0) + \int_{t_0}^{t} (\psi - \delta) I(k) \mathrm{e}^{r(k-t_0)}\mathrm{d}k), \quad 0 < R(t) < +\infty, \\
D(t) &= \mathrm{e}^{-r(t-t_0)}(D(t_0) + \int_{t_0}^{t} (\delta - \psi) I(k) \mathrm{e}^{r(k-t_0)}\mathrm{d}k), \quad 0 < D(t) < +\infty,
\end{aligned}$$

where "e" is the exponential or Euler function. We know that the total population is the sum of all cases, that is,

$$N(t) = S(t) + I(t) + R(t) + D(t),$$

which is presented as

$$\begin{aligned}
N(t) &= S(t_0) + \mathrm{e}^{-\beta \int_{t_0}^{t} I(k)\mathrm{d}k} + I(t_0) + \mathrm{e}^{\int_{t_0}^{t} (\beta S(k) - (\delta+\psi))\mathrm{d}k} \\
&\quad + \mathrm{e}^{-r(t-t_0)} \left(R(t_0) + \int_{t_0}^{t} (\psi - \delta) I(k) \mathrm{e}^{r(k-t_0)}\mathrm{d}k \right) \\
&\quad + \mathrm{e}^{-r(t-t_0)} \left(D(t_0) + \int_{t_0}^{t} (\delta - \psi) I(k) \mathrm{e}^{r(k-t_0)}\mathrm{d}k \right).
\end{aligned}$$

From the above expression of $N(t)$, we can conclude that the solution of the total population is always positive because the initial populations are positive and the solutions $S(t)$, $I(t)$, $R(t)$, and $D(t)$ are positively bounded. Therefore, $0 < N(t) < +\infty$. Thus, the total population is always positively bounded at any time $t \in [0, \infty)$ for both expressions presented in (1) and (2).

3. Results and Analysis

This section presents a comprehensive analysis of our novel SIRD model, including the analytical solution using the LADM and the examination of fuzzy-valued solutions.

3.1. Analytical Solution Using the LADM

To obtain the analytical solution of the new fractional epidemic model stated in (3), we employ the LADM, following a similar approach to that used in [19]. The values of $S(t)$, $I(t)$, $R(t)$, and $D(t)$ are obtained through an iterative procedure formulated as

$$\begin{aligned}
S(k+1) &= \mathcal{L}^{-1}(-\beta / s^{\alpha 1} \mathcal{L}(A_k)) \\
I(k+1) &= \mathcal{L}^{-1}(\beta / s^{\alpha 2} \mathcal{L}(A_k) - (\delta + \psi) / s^{\alpha 2} \mathcal{L}(I_k)) \\
R(k+1) &= \mathcal{L}^{-1}((\delta - \psi) / s^{\alpha 3} \mathcal{L}(I_k) - (\psi / s^{\alpha 3} \mathcal{L}(R_k))) \\
D(k+1) &= \mathcal{L}^{-1}((\psi - \delta) / s^{\alpha 4} \mathcal{L}(I_k) - (\psi) / s^{\alpha 4} \mathcal{L}(D_k)).
\end{aligned} \tag{4}$$

In the expressions stated in (4), A_k denotes an Adomian polynomial, which is defined as

$$A_k = \frac{1}{k!}\frac{D^k}{\lambda^k}\sum_{l=0}^{k}\left(\lambda^l S_l\, \lambda^l I_l\right)\Big|_{\lambda=0}.$$

These polynomials are generated iteratively, which is a characteristic feature of the Adomian decomposition method. This method allows us to approximate the solution of a differential equation by dividing it into a series of simpler problems. At each iteration, the polynomial A_k is calculated based on the solution from the previous iteration (or the initial guess for $k = 0$) and the non-linear part of the differential equation. This iterative process continues until the solution converges or a predetermined maximum number of iterations is reached. For example: $A_0 = S_0 I_0$, $A_1 = S_0 I_1 + S_1 I_0$, $A_2 = S_0 I_2 + S_1 I_1 + S_2 I_0$, and so on. In our model, the polynomials A_k are used to construct the iterative solutions for the fractional epidemic model functions $S(t)$, $I(t)$, $R(t)$, and $D(t)$, represented as infinite series given as

$$S(t) = \sum_{k=0}^{\infty} S(k), \quad I(t) = \sum_{k=0}^{\infty} I(k), \quad R(t) = \sum_{k=0}^{\infty} R(k), \quad D(t) = \sum_{k=0}^{\infty} D(k).$$

Concerning the error term and convergence analysis, it is important to note that this study does not encompass a detailed analysis of the error term or the convergence of the LADM. However, the convergence properties of the LADM have been extensively studied and verified in related works [19]. Although an explicit analysis of the error term is not included in this article, the LADM is recognized in the scientific community as an effective approach for obtaining accurate and reliable numerical solutions in fractional calculus. Our study primarily focuses on the development of the new fractional epidemic model and the investigation of its dynamics under various conditions.

Compared to homotopy methods, the LADM offers the advantage of simplicity in terms of implementation, and it is well-suited for problems involving non-linearities. Moreover, the LADM does not require the presence of a homotopy parameter, which is needed in homotopy methods. The absence of this parameter simplifies the analysis and makes the LADM a more straightforward tool for our investigation.

We suggest that further research could explore the specific analysis of the error term and convergence properties in the context of our proposed model, potentially including a direct comparison of the LADM and homotopy methods in the context of fractional epidemic models.

3.2. Fuzzy-Valued Solutions

For the FSDE given in (2), after assigning the values to all the parameters, by applying the LADM up to fourth order and setting the fractional orders $\alpha_1 = \alpha_2 = \alpha_3 = \alpha_4 = 1$, we obtain crisp (non-fuzzy) solutions. Then, these crisp solutions are transformed into fuzzy-valued solutions by multiplying them with the fuzzy numbers $(0.75 + 0.25r, 1.125 - 0.125r)$, where $r \in [0, 1]$ is a measure of uncertainty or fuzziness, and presented as

$$\begin{aligned}
\widetilde{S}(t) &= (0.75 + 0.25r, 1.125 - 0.125r)\left(350 - 98t + 10.045t^2 + 0.7771t^3 - 0.31925t^4\right)\\
\widetilde{I}(t) &= (0.75 + 0.25r, 1.125 - 0.125r)\left(400 + 30t - 12.595t^2 - 0.0633t^3 + 0.32195t^4\right)\\
\widetilde{R}(t) &= (0.75 + 0.25r, 1.125 - 0.125r)\left(400 - 28t + 1.270t^2 - 0.0758t^3 + 0.00136t^4\right)\\
\widetilde{D}(t) &= (0.75 + 0.25r, 1.125 - 0.125r)\left(350 - 32t + 1.130t^2 + 0.0118t^3 - 0.00008t^4\right).
\end{aligned}$$

The stability of our solutions is demonstrated using a complex plane portrait, as shown in Figure 2. The non-fuzzy, non-fractional numbers of $S(t)$, $I(t)$, $R(t)$, and $D(t)$ for the time interval $t \in [0, 1]$ are presented in Table 1. The corresponding graphical representation, covering a more extended time, with $t \in [0, 100]$, is displayed in Figure 3. The 2D representations of the non-fuzzy fractional cases $S(t)$, $I(t)$, $R(t)$, and $D(t)$ are respectively illustrated in Figures 4–7.

Table 1. Crisp valued and non-fractional solutions for $S(t)$, $I(t)$, $R(t)$, and $D(t)$ with $t \in [0,1]$.

t	$S(t)$	$I(t)$	$R(t)$	$D(t)$
0.0	350.000	400.000	400.000	350.000
0.1	340.301	402.874	397.213	346.811
0.2	330.808	405.496	394.450	343.645
0.3	321.522	407.867	391.712	340.502
0.4	312.449	409.989	388.998	337.382
0.5	303.588	411.863	386.308	334.284
0.6	294.943	413.494	383.641	331.209
0.7	286.512	414.884	380.997	328.158
0.8	278.296	416.039	378.375	325.129
0.9	270.293	416.963	375.774	322.124
1.0	262.503	417.664	373.196	319.142

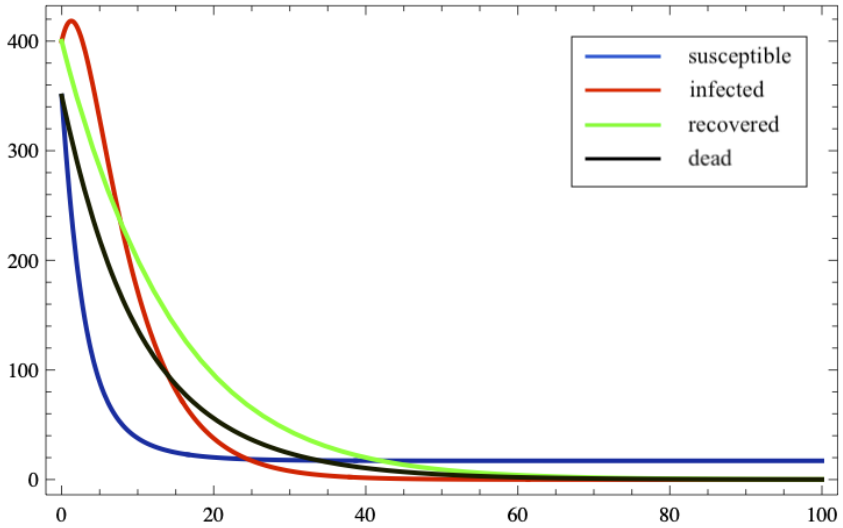

Figure 3. Ordinary differential model for $S(t)$, $I(t)$, $R(t)$, and $D(t)$ with $t \in [0,100]$ and $\alpha = 1$.

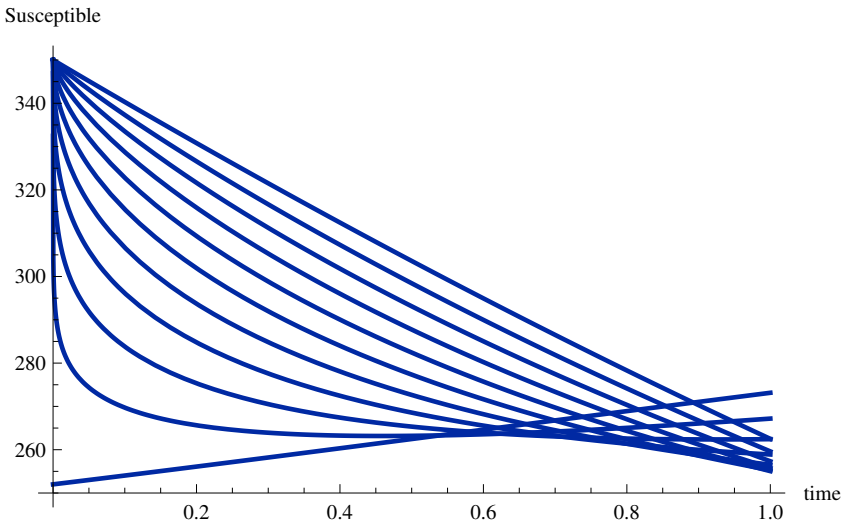

Figure 4. Fractional model for $S(t)$ with $t \in [0,1]$ and $\alpha \in [0,1]$.

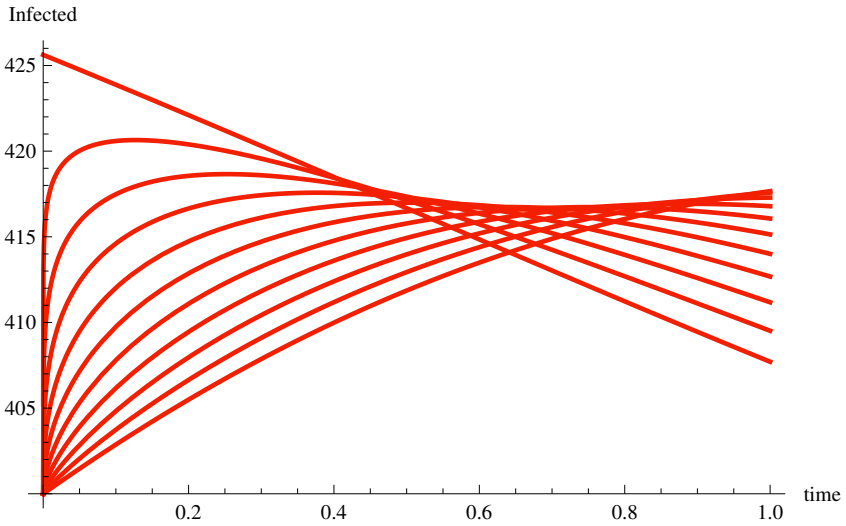

Figure 5. Fractional model for $I(t)$ with $t \in [0,1]$ and $\alpha \in [0,1]$.

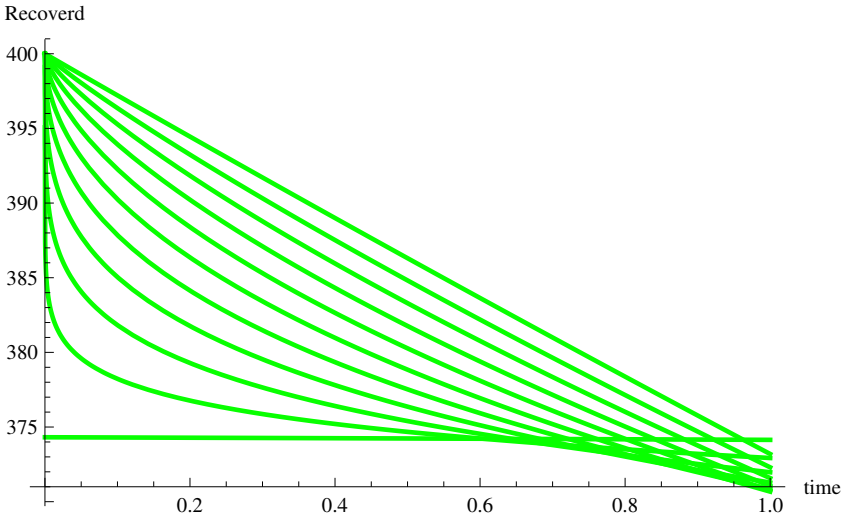

Figure 6. Fractional model for $R(t)$ with $t \in [0,1]$ and $\alpha \in [0,1]$.

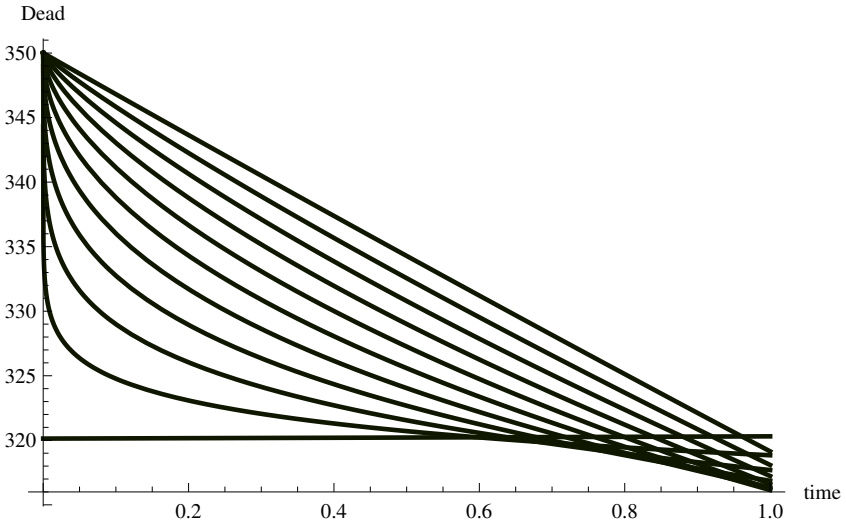

Figure 7. Fractional model for $D(t)$ with $t \in [0,1]$ and $\alpha \in [0,1]$.

Now, based on the fuzzy-valued solutions given by

$$\begin{aligned}
\widetilde{S}(t) &= 350 - \frac{98\,t^{\alpha}}{\Gamma(1+\alpha)} + \frac{20.09\,t^{2\alpha}}{\Gamma(1+2\alpha)} + \frac{0.5464\,t^{3\alpha}}{\Gamma(1+3\alpha)} + \frac{2.058\,t^{3\alpha}\Gamma(1+2\alpha)}{\Gamma(1+\alpha)^2\Gamma(1+3\alpha)} \\
&\quad - \frac{1.0683\,t^{4\alpha}}{\Gamma(1+4\alpha)} - \frac{0.0720\,t^{4\alpha}\Gamma(1+2\alpha)}{\Gamma(1+\alpha)^2\Gamma(1+4\alpha)} - \frac{2.1499\,t^{4\alpha}\Gamma(1+3\alpha)}{\Gamma(1+\alpha)\Gamma(1+2\alpha)\Gamma(1+4\alpha)} \\
\widetilde{I}(t) &= 400 + \frac{30\,t^{\alpha}}{\Gamma(1+\alpha)} - \frac{25.19\,t^{2\alpha}}{\Gamma(1+2\alpha)} + \frac{3.7359\,t^{3\alpha}}{\Gamma(1+3\alpha)} - \frac{2.058\,t^{3\alpha}\Gamma(1+2\alpha)}{\Gamma(1+\alpha)^2\Gamma(1+3\alpha)} \\
&\quad + \frac{0.4332\,t^{4\alpha}}{\Gamma(1+4\alpha)} + \frac{0.4219\,t^{4\alpha}\Gamma(1+2\alpha)}{\Gamma(1+\alpha)^2\Gamma(1+4\alpha)} + \frac{2.1499\,t^{4\alpha}\Gamma(1+3\alpha)}{\Gamma(1+\alpha)\Gamma(1+2\alpha)\Gamma(1+4\alpha)} \\
\widetilde{R}(t) &= 400 - \frac{28\,t^{\alpha}}{\Gamma(1+\alpha)} + \frac{2.54\,t^{2\alpha}}{\Gamma(1+2\alpha)} - \frac{0.4551\,t^{3\alpha}}{\Gamma(1+3\alpha)} + \frac{0.0738\,t^{4\alpha}}{\Gamma(1+4\alpha)} \\
&\quad - \frac{0.0206\,t^{4\alpha}\Gamma(1+2\alpha)}{\Gamma(1+\alpha)^2\Gamma(1+4\alpha)} \\
\widetilde{D}(t) &= 350 - \frac{32\,t^{\alpha}}{\Gamma(1+\alpha)} + \frac{2.26\,t^{2\alpha}}{\Gamma(1+2\alpha)} + \frac{0.0711\,t^{3\alpha}}{\Gamma(1+3\alpha)} - \frac{0.0430\,t^{4\alpha}}{\Gamma(1+4\alpha)} \\
&\quad + \frac{0.0206\,t^{4\alpha}\Gamma(1+2\alpha)}{\Gamma(1+\alpha)^2\Gamma(1+4\alpha)},
\end{aligned}$$

we extend our analysis to the cases of the infected, recovered, and dead populations for $t \in [0,1]$, considering varying values of α in two ranges: $[0, 0.4]$ and $[0.5, 1]$.

The 3D non-fuzzy population data for each group are visualized and tabulated. Specifically, the susceptible cases are detailed in Tables 2 and 3 and Figure 8. Infected cases are presented in Tables 4 and 5 and Figure 9. Recovered cases are depicted in Tables 6 and 7 and Figure 10, while deceased cases are outlined in Tables 8 and 9 and Figure 11. All these representations correspond to the fractional orders $\alpha_i \in [0,1]$, for $i \in \{1,2,3,4\}$.

Figure 12 provides the complete visualization of the SIRD model for non-fuzzy fractional cases. For the fuzzy-valued cases, graphical representations are provided for varying fuzziness degrees $r \in [0,1]$. For a fixed common fractional order $\alpha_i = 1$, with $i \in \{1,2,3,4\}$, the plots for $S(t)$, $I(t)$, $R(t)$, and $D(t)$ are shown in Figures 13–16 over the time interval $t \in [0,1]$. Similarly, for varying fractional orders $\alpha_i \in [0,1]$, with $i \in \{1,2,3,4\}$, the fuzzy-valued plots for $S(t)$, $I(t)$, $R(t)$, and $D(t)$ are provided in Figures 17–20, respectively.

Table 2. Cases of susceptible population for $t \in [0,1]$ and $\alpha \in [0, 0.4]$.

t	$\alpha = 0$	$\alpha = 0.1$	$\alpha = 0.2$	$\alpha = 0.3$	$\alpha = 0.4$
0	271.404	271.404	271.404	271.404	271.404
0.1	350.000	281.949	277.988	275.584	273.837
0.2	350.000	291.836	284.654	280.134	276.778
0.3	350.000	301.077	291.384	285.024	280.187
0.4	350.000	309.547	298.109	290.224	284.056
0.5	350.000	317.094	304.690	295.653	288.350
0.6	350.000	323.626	310.962	301.181	292.987
0.7	350.000	329.136	316.784	306.658	297.848
0.8	350.000	333.682	322.058	311.944	302.796
0.9	350.000	337.364	326.735	316.925	307.701
1	350.000	340.301	330.808	321.522	312.449

Table 3. Cases of susceptible population for $t \in [0,1]$ and $\alpha \in [0.5,1]$.

t	$\alpha = 0.5$	$\alpha = 0.6$	$\alpha = 0.7$	$\alpha = 0.8$	$\alpha = 0.9$	$\alpha = 1$
0	271.404	271.404	271.404	271.404	271.404	271.404
0.1	272.457	271.314	270.335	269.479	268.716	268.028
0.2	274.086	271.825	269.871	268.143	266.593	265.184
0.3	276.244	272.893	269.967	267.36	265.004	262.848
0.4	278.932	274.519	270.624	267.126	263.941	261.012
0.5	282.146	276.716	271.865	267.467	263.433	259.699
0.6	285.849	279.482	273.711	268.419	263.521	258.955
0.7	289.959	282.775	276.155	270.003	264.248	258.835
0.8	294.369	286.52	279.156	272.210	265.632	259.38
0.9	298.953	290.614	282.64	274.998	267.661	260.608
1	303.588	294.943	286.512	278.296	270.293	262.503

Table 4. Cases of infected population for $t \in [0,1]$ and $\alpha \in [0,0.4]$.

t	$\alpha = 0$	$\alpha = 0.1$	$\alpha = 0.2$	$\alpha = 0.3$	$\alpha = 0.4$
0	409.493	409.493	409.493	409.493	409.493
0.1	400.000	410.036	409.913	409.811	409.725
0.2	400.000	410.305	410.395	410.321	410.207
0.3	400.000	410.061	410.705	410.860	410.838
0.4	400.000	409.316	410.672	411.232	411.449
0.5	400.000	408.233	410.260	411.311	411.881
0.6	400.000	407.006	409.532	411.061	412.039
0.7	400.000	405.784	408.593	410.517	411.891
0.8	400.000	404.663	407.553	409.750	411.462
0.9	400.000	403.689	406.500	408.841	410.806
1	400.000	402.874	405.496	407.867	409.989

Table 5. Cases of infected population for $t \in [0,1]$ and $\alpha \in [0.5,1]$.

t	$\alpha = 0.5$	$\alpha = 0.6$	$\alpha = 0.7$	$\alpha = 0.8$	$\alpha = 0.9$	$\alpha = 1$
0	409.493	409.493	409.493	409.493	409.493	409.493
0.1	409.653	409.589	409.533	409.483	409.437	409.396
0.2	410.082	409.958	409.838	409.724	409.616	409.514
0.3	410.736	410.593	410.429	410.256	410.079	409.904
0.4	411.481	411.403	411.256	411.063	410.843	410.604
0.5	412.163	412.252	412.208	412.069	411.859	411.598
0.6	412.651	413.000	413.153	413.152	413.031	412.816
0.7	412.868	413.539	413.964	414.185	414.238	414.148
0.8	412.793	413.807	414.550	415.057	415.356	415.472
0.9	412.443	413.786	414.861	415.689	416.288	416.674
1	411.863	413.494	414.884	416.039	416.963	417.664

Table 6. Cases of recovered population for $t \in [0,1]$ and $\alpha \in [0,0.4]$.

t	$\alpha = 0$	$\alpha = 0.1$	$\alpha = 0.2$	$\alpha = 0.3$	$\alpha = 0.4$
0.0	374.138	374.138	374.138	374.138	374.138
0.1	400.000	378.137	376.667	375.765	375.104
0.2	400.000	381.779	379.223	377.573	376.328
0.3	400.000	385.021	381.727	379.490	377.748
0.4	400.000	387.844	384.118	381.452	379.307
0.5	400.000	390.252	386.349	383.403	380.951
0.6	400.000	392.270	388.389	385.296	382.633
0.7	400.000	393.931	390.220	387.096	384.312
0.8	400.000	395.279	391.836	388.776	385.950
0.9	400.000	396.359	393.243	390.318	387.519
1.0	400.000	397.213	394.450	391.712	388.998

Table 7. Cases of recovered population for $t \in [0,1]$ and $\alpha \in [0.5,1]$.

t	$\alpha = 0.5$	$\alpha = 0.6$	$\alpha = 0.7$	$\alpha = 0.8$	$\alpha = 0.9$	$\alpha = 1$
0.0	374.138	374.138	374.138	374.138	374.138	374.138
0.1	374.581	374.145	373.771	373.444	373.151	372.887
0.2	375.318	374.462	373.717	373.055	372.458	371.914
0.3	376.301	375.053	373.949	372.956	372.051	371.217
0.4	377.482	375.878	374.439	373.126	371.917	370.791
0.5	378.814	376.900	375.155	373.543	372.040	370.627
0.6	380.254	378.080	376.067	374.181	372.402	370.712
0.7	381.759	379.380	377.140	375.012	372.981	371.032
0.8	383.291	380.763	378.341	376.009	373.753	371.566
0.9	384.817	382.194	379.637	377.139	374.694	372.296
1.0	386.308	383.641	380.997	378.375	375.774	373.196

Table 8. Cases of dead population for $t \in [0,1]$ and $\alpha \in [0,0.4]$.

t	$\alpha = 0$	$\alpha = 0.1$	$\alpha = 0.2$	$\alpha = 0.3$	$\alpha = 0.4$
0.0	320.309	320.309	320.309	320.309	320.309
0.1	350.000	324.864	323.184	322.154	321.401
0.2	350.000	329.040	326.102	324.210	322.784
0.3	350.000	332.773	328.977	326.402	324.400
0.4	350.000	336.030	331.732	328.658	326.185
0.5	350.000	338.809	334.308	330.909	328.079
0.6	350.000	341.134	336.664	333.097	330.023
0.7	350.000	343.046	338.777	335.178	331.965
0.8	350.000	344.595	340.640	337.118	333.860
0.9	350.000	345.833	342.258	338.896	335.675
1.0	350.000	346.811	343.645	340.502	337.382

Table 9. Cases of dead population for $t \in [0,1]$ and $\alpha \in [0.5,1]$.

t	$\alpha = 0.5$	$\alpha = 0.6$	$\alpha = 0.7$	$\alpha = 0.8$	$\alpha = 0.9$	$\alpha = 1$
0.0	320.309	320.309	320.309	320.309	320.309	320.309
0.1	320.804	320.309	319.884	319.511	319.179	318.879
0.2	321.629	320.653	319.803	319.049	318.370	317.752
0.3	322.739	321.309	320.046	318.912	317.879	316.929
0.4	324.085	322.241	320.588	319.084	317.699	316.412
0.5	325.614	323.409	321.399	319.545	317.818	316.197
0.6	327.276	324.767	322.443	320.269	318.219	316.275
0.7	329.018	326.270	323.682	321.225	318.880	316.632
0.8	330.793	327.873	325.075	322.379	319.773	317.246
0.9	332.560	329.532	326.580	323.693	320.866	318.093
1.0	334.284	331.209	328.158	325.129	322.124	319.142

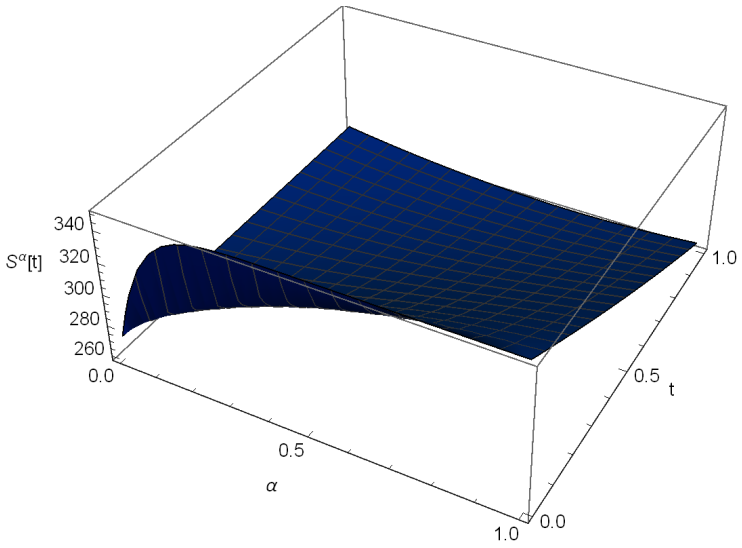

Figure 8. Fractional model $S(t)$ for $t \in [0,1]$ and $\alpha \in [0,1]$.

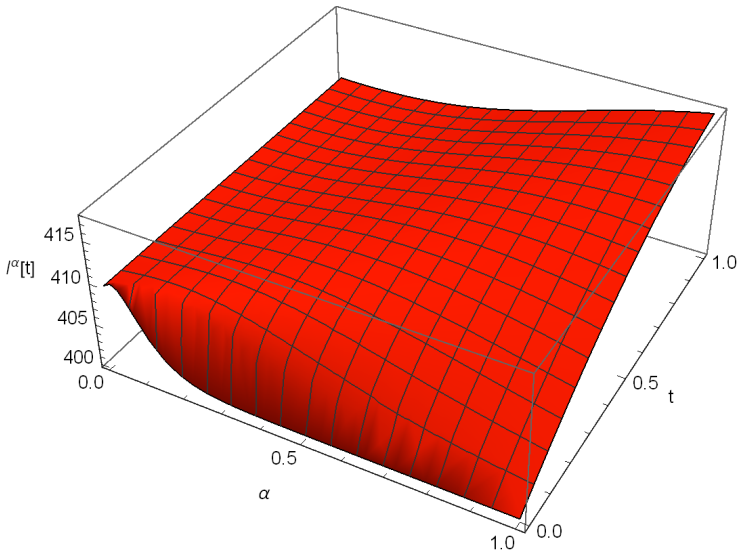

Figure 9. Fractional model $I(t)$ for $t \in [0,1]$ and $\alpha \in [0,1]$.

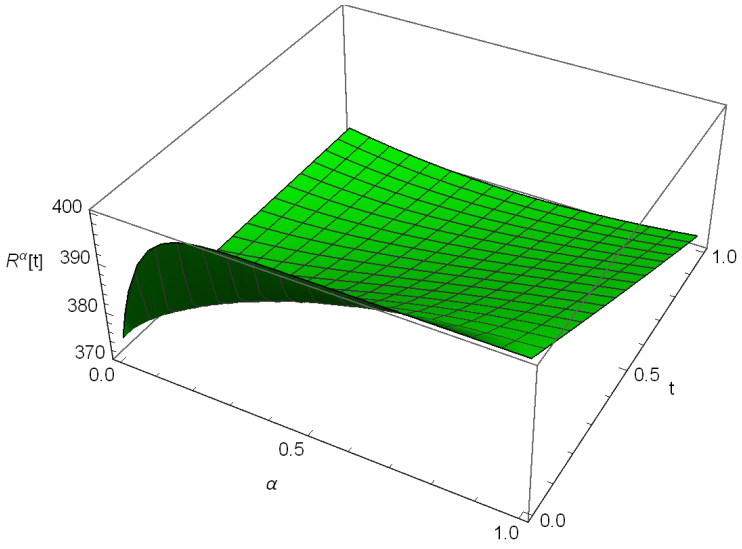

Figure 10. Fractional model $R(t)$ for $t \in [0,1]$ and $\alpha \in [0,1]$.

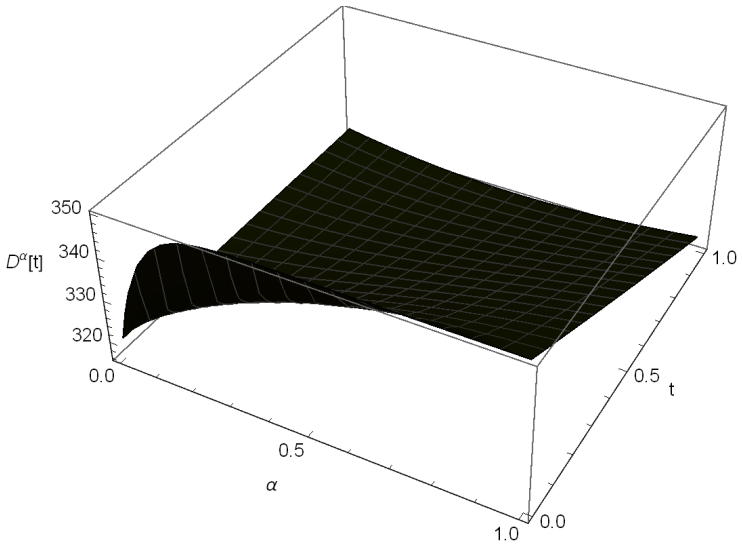

Figure 11. Fractional model $D(t)$ for $t \in [0,1]$ and $\alpha \in [0,1]$.

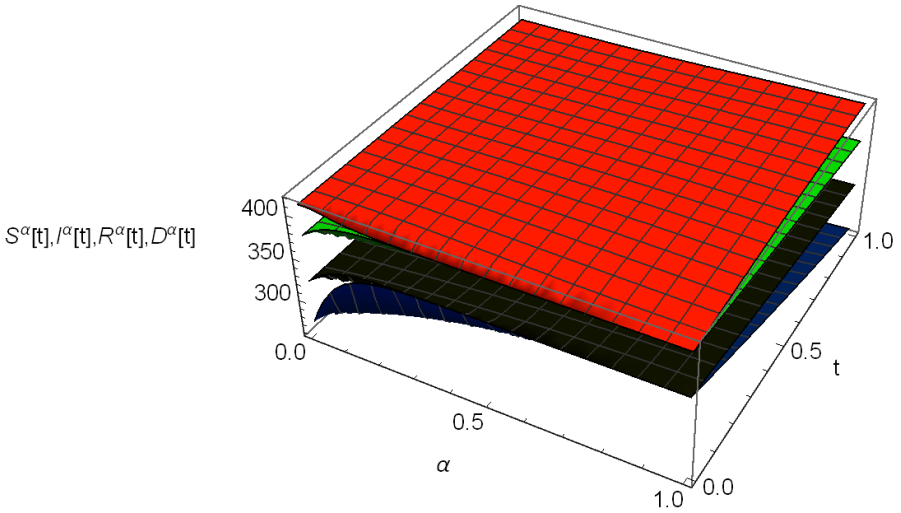

Figure 12. Fractional differential SIRD model of $S(t)$, $I(t)$, $R(t)$, and $D(t)$ for $t \in [0,100]$ and $\alpha \in [0,1]$.

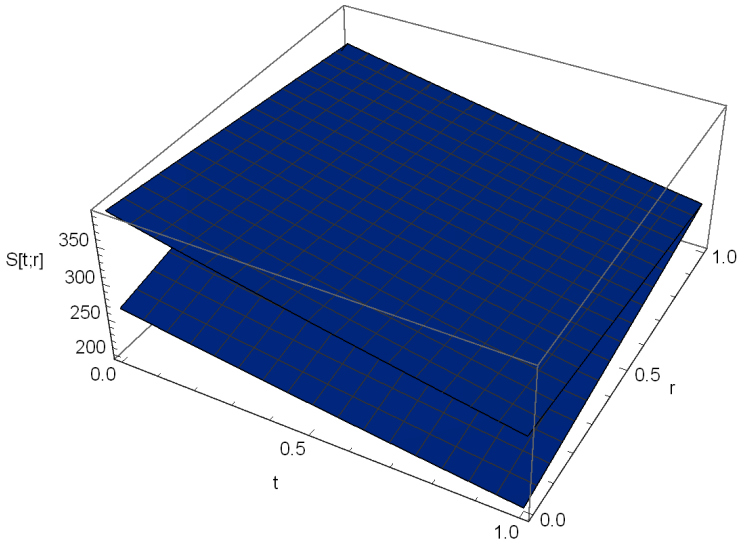

Figure 13. Fractional model $S(t)$ for $t \in [0,1]$ and $r \in [0,1]$.

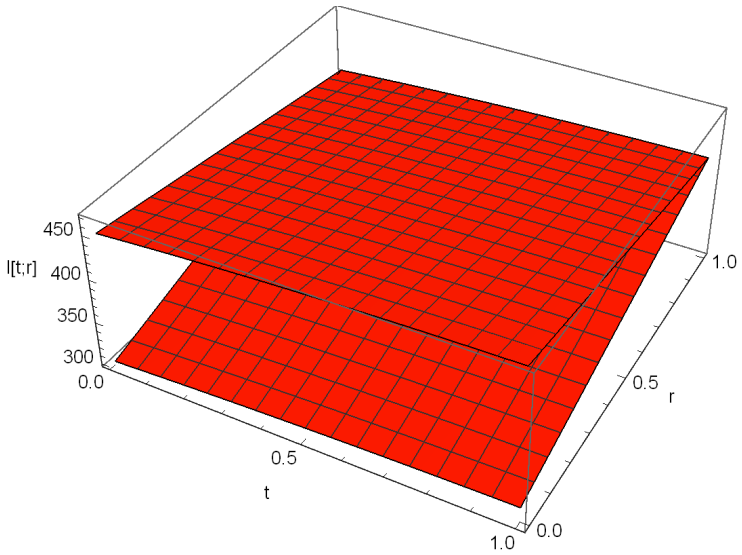

Figure 14. Fractional model $I(t)$ for $t \in [0,1]$ and $r \in [0,1]$.

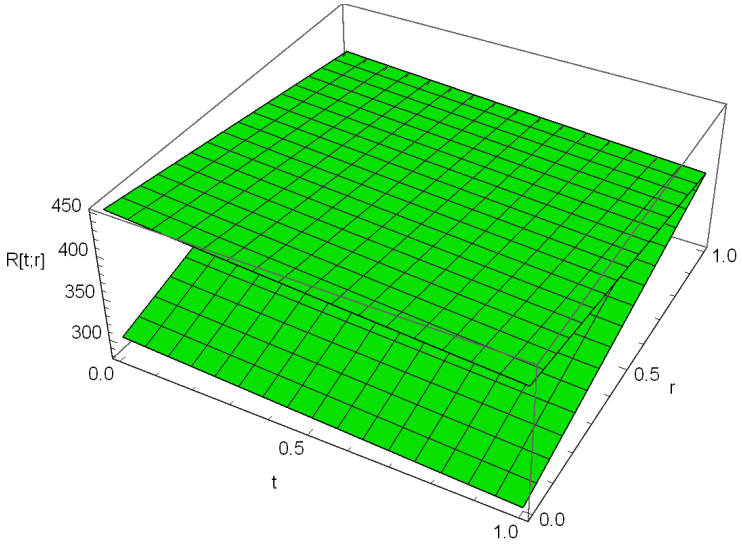

Figure 15. Fractional model $R(t)$ for $t \in [0,1]$ and $r \in [0,1]$.

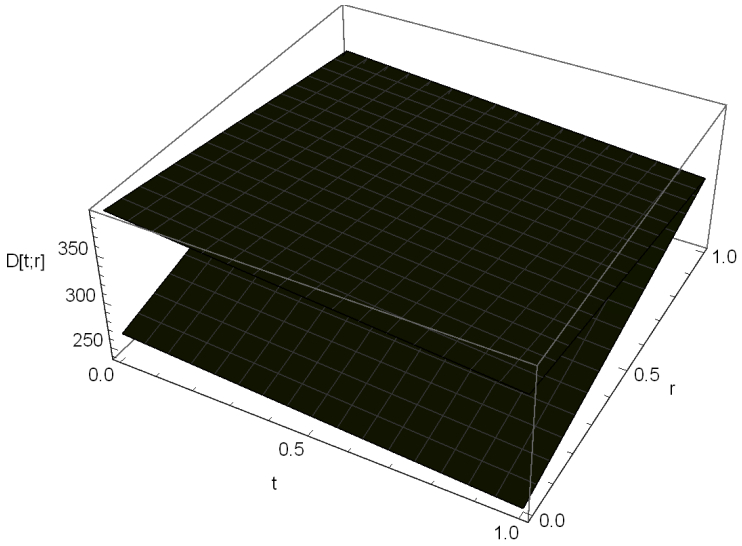

Figure 16. Fractional model $D(t)$ for $t \in [0,1]$ and $r \in [0,1]$.

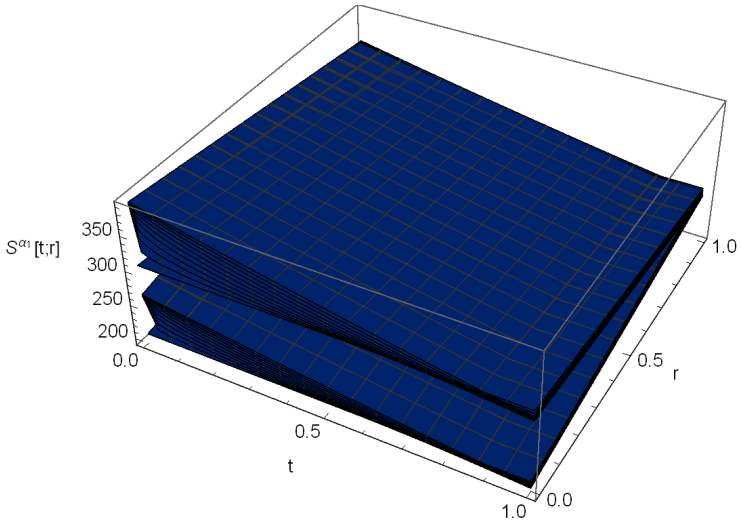

Figure 17. Fuzzy fractional model $S^{\alpha}(t)$ for $t \in [0,1]$ and $\alpha \in [0,1]$.

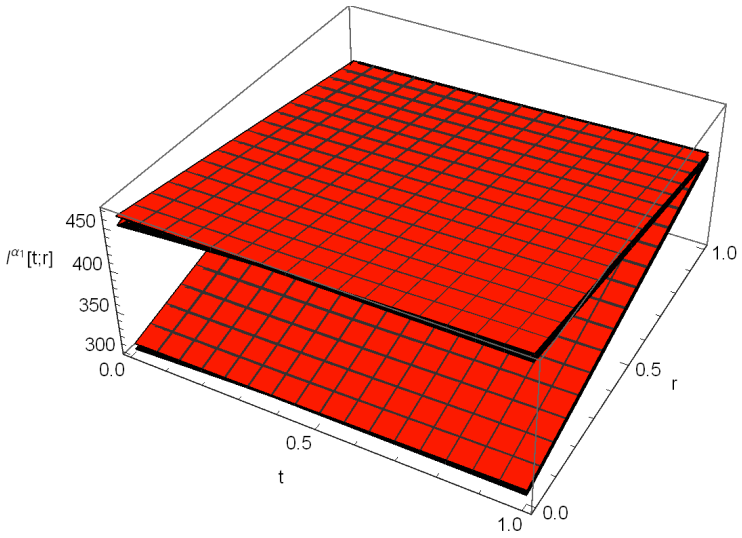

Figure 18. Fuzzy fractional model $I^{\alpha}(t)$ for $t \in [0,1]$ and $\alpha \in [0,1]$.

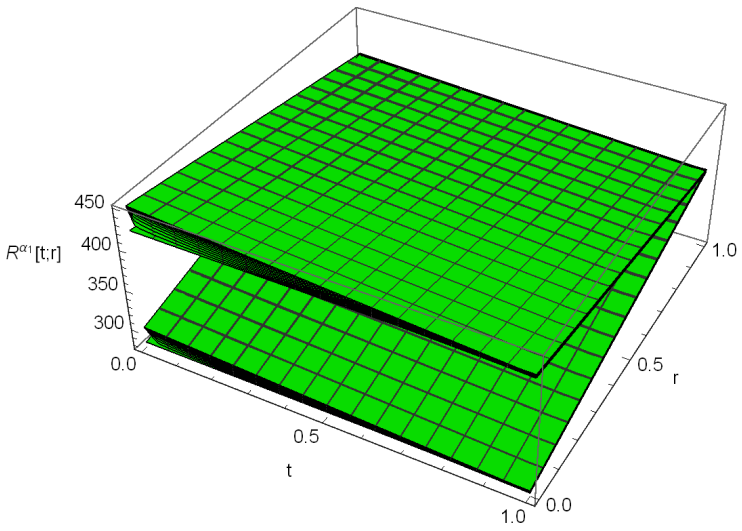

Figure 19. Fuzzy fractional model $R^{\alpha}(t)$ for $t \in [0,1]$ and $\alpha \in [0,1]$.

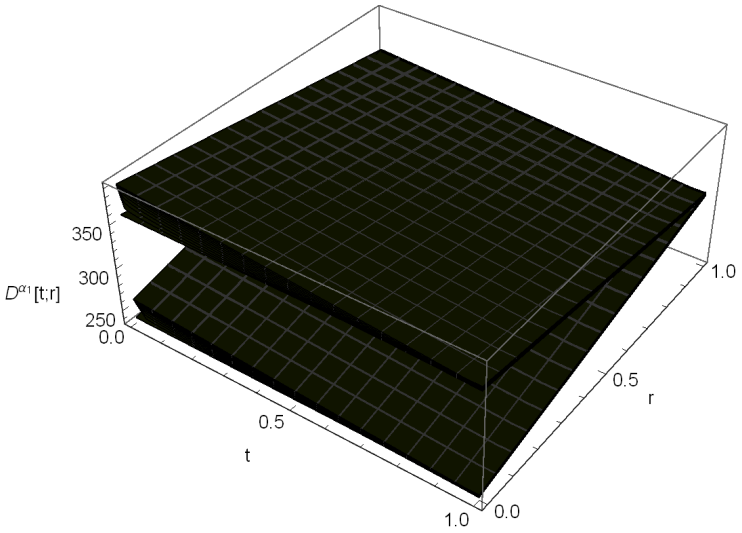

Figure 20. Fuzzy fractional model $D^{\alpha}(t)$ for $t \in [0,1]$ and $\alpha \in [0,1]$.

Note that the decay observed in all compartments $S(t)$, $I(t)$, $R(t)$, and $D(t)$ suggests a decline in $S(t)$, $I(t)$, and $R(t)$, as well as a decrease in $D(t)$, over time t. This can be attributed to various factors such as the implementation of preventive measures, the development of immunity, and effective medical interventions.

The faster decay observed in $S(t)$ indicates a decrease in the number of individuals who are susceptible to the disease. This could be a result of interventions such as vaccination campaigns or public health measures that reduce the transmission of the disease and protect individuals from becoming infected. In addition, the slower decay observed in $R(t)$ suggests a longer duration of the recovery process. This may be due to the time required for individuals to fully recover from the disease and regain their health.

Regarding the non-fuzzy fractional cases, the similar decaying behaviors of $S(t)$, $R(t)$, and $D(t)$ indicate that these compartments are influenced by similar factors and follow similar trends over time. However, the distinct behavior of $I(t)$ highlights the complexity of the disease dynamics. For lower values of the fractional order α, the number of cases tends to increase, indicating a higher transmission rate or a slower recovery process. In contrast, for higher values of α, the number of cases decreases, suggesting a reduced transmission rate or a more efficient recovery process.

When considering the model with fuzzy values, the behaviors of the different compartments undergo relative changes compared to the crisp-valued model. In the fuzzy-valued cases, the compartments $S(t)$, $I(t)$, $R(t)$, and $D(t)$ exhibit different dynamics compared to the non-fuzzy fractional cases.

For the fuzzy-valued $S(t)$, the behavior is influenced by the degree of fuzziness rather than by a specific fractional order. This indicates that the uncertainty in the susceptible population affects the spread of the disease, with different levels of fuzziness leading to different patterns of disease transmission.

Similarly, the fuzzy-valued $I(t)$, $R(t)$, and $D(t)$ show different behaviors compared to their non-fuzzy counterparts. The presence of fuzziness introduces additional variability in the number of infections, recoveries, and deaths, reflecting the uncertainty in the disease progression and outcomes. These changes in behavior highlight the importance of considering fuzziness in epidemiological models.

Overall, the inclusion of fuzzy values in the model enhances our understanding of the uncertainties associated with the disease's spread and outcomes, enabling more robust decision-making in public health interventions and policy development.

4. Conclusions

In conclusion, our study presented a novel susceptible, infected, recovered, and dead model that effectively captures the epidemic spread dynamics. We identified equilibrium states and computed the basic reproduction number, also confirming the asymptotic stability of the solutions through stability analysis. The use of a fourth-order Laplace-Adomian decomposition method provided accurate and reliable numerical solutions, demonstrating a fourth-order convergence.

The inclusion of fuzziness in our model deepened our understanding of population dynamics under various conditions. By taking into account different levels of uncertainty and fractional orders, we gained insights into the evolution of susceptible, infected, recovered, and deceased populations over time. The incorporation of fuzziness enhanced the model's ability to represent the complexity and inherent uncertainty present in real-world epidemic scenarios.

Looking forward, there are several avenues for future research. Firstly, we plan to conduct a more in-depth analysis of the positivity and boundedness of the solutions, further validating the feasibility of the model. This analysis will ensure that the population compartments remain non-negative and finite over time, strengthening the model's applicability. Furthermore, additional investigations could explore the impact of delay differential systems on epidemic dynamics. Incorporating delays will offer a more comprehensive understanding of temporal dynamics and enable the development of strategies to mitigate the effects of delays on public health responses.

By pursuing these research directions, we aim to significantly contribute to the understanding and effective management of public health crises, including pandemics. Our work provides a solid foundation for future studies and offers valuable insights into the behavior and control of epidemic outbreaks.

Author Contributions: Conceptualization, K.U., B.P., V.L., P.B.D. and C.C.; formal analysis, K.U., B.P., V.L., P.B.D. and C.C.; investigation, K.U., B.P., V.L., P.B.D. and C.C.; methodology, K.U., B.P., V.L., P.B.D. and C.C.; writing—original draft, K.U., B.P., P.B.D. and C.C.; writing—review and editing, V.L. All authors have read and agreed to the published version of the manuscript.

Funding: This research was funded partially by project grant Fondecyt 1200525 (V.L.) from the National Agency for Research and Development (ANID) of the Chilean government under the Ministry of Science, Technology, Knowledge, and Innovation; and by Portuguese funds through the CMAT-Research Centre of Mathematics of University of Minho - within references UIDB/00013/2020, UIDP/00013/2020 (C.C.).

Institutional Review Board Statement: Not applicable.

Informed Consent Statement: Not applicable.

Data Availability Statement: Not applicable.

Acknowledgments: The authors would like to thank the editors and reviewers for their constructive comments, which led to improvements in the presentation of the manuscript.

Conflicts of Interest: There are no conflict of interest declared by the authors.

References

1. Allen, L.J.S. *An Introduction to Mathematical Biology*; Prentice-Hall: Hoboken, NJ, USA, 2007.
2. Li, X.Z.; Yang, J.; Martcheva, M. *Age Structured Epidemic Modeling*; Springer: New York, NY, USA, 2020.
3. Mollison, D. *Epidemic Models: Their Structure and Relation to Data*; Cambridge University Press: Cambridge, UK, 1995.
4. Altaf, K.M.; Sajjad, U.; Muhammad, F. Fractional order SEIR model with generalized incidence rate. *Aims Math.* **2020**, *5*, 2843–2857. [CrossRef]
5. Rangasamy, M.; Chesneau, C.; Martin-Barreiro, C.; Leiva, V. On a novel dynamics of SEIR epidemic models with a potential application to COVID-19. *Symmetry* **2022**, *14*, 1436. [CrossRef]
6. Esquivel, M.L.; Krasii, N.P.; Guerreiro, G.R.; Patricio, P. The multi-compartment SI (RD) model with regime switching: An application to COVID-19 pandemic. *Symmetry* **2021**, *13*, 2427. [CrossRef]
7. Sinan, M.; Alharthi, N.H. Mathematical analysis of fractal-fractional mathematical model of COVID-19. *Fractal Fract.* **2023**, *7*, 358. [CrossRef]

8. Antangana, A.; Baleanu, D. New fractional derivative with non-local and non-singular kernel theory and application to heat transfer model. *Therm. Sci.* **2016**, *20*, 763–769. [CrossRef]
9. Brauer, F.; Castillo-Chavez, C.; Castillo-Chavez, C. *Mathematical Models in Population Biology and Epidemiology*; Springer: New York, NY, USA, 2001.
10. Murray, J.D. *Mathematical Biology I: An Introduction*; Springer: New York, NY, USA, 2002.
11. Chen-Charpentier, B. Delays and exposed populations in infection models. *Mathematics* **2023**, *11*, 1919. [CrossRef]
12. Wang, L.X. *Adaptive Fuzzy Systems and Control: Design and Stability Analysis*; Prentice-Hall: New York, NY, USA, 1994.
13. Terano, T.; Asai, K.; Sugeno, M. *Fuzzy Systems Theory and Its Applications*; Academic Press: New York, NY, USA, 1992.
14. Zadeh, L.A. Fuzzy sets. *Inf. Control.* **1965**, *8*, 338–353. [CrossRef]
15. Bukley, J.J.; Feuring, T. Fuzzy differential equations. *Fuzzy Sets Syst.* **2000**, *110*, 43–54. [CrossRef]
16. Abbasbandy, S. Extended Newton's method for a system of nonlinear equations by modified Adomian decomposition method. *Appl. Math. Comput.* **2005**, *170*, 648–656. [CrossRef]
17. Makinde, O.D. Adomian decomposition approach to a SIR epidemic model with constant vaccination strategy. *Appl. Math. Comput.* **2007**, *184*, 842–848. [CrossRef]
18. Ongun, M.Y. The Laplace Adomian decomposition method for solving a model for HIV infection of $CD4^+$ T-cells. *Math. Comput. Model* **2011**, *53*, 597–603. [CrossRef]
19. Farman, M.; Saleem, U.F.; Ahmad, A.; Ahamed, M.O. Analysis and numerical solution of SEIR epidemic model of measles with non-integer time fractional derivatives by using Laplace Adomian decomposition method. *Ain Shams Eng. J.* **2018**, *9*, 3391–3397. [CrossRef]
20. Umapathy, K.; Palanivelu, B.; Jayaraj, R.; Baleanu, D.; Dhandapani, P.B. On the decomposition and analysis of novel simultaneous SEIQR epidemic model. *Aims Math.* **2023**, *10*, 5918–5933.
21. Chebotaeva, V.; Vasquez, P.A. Erlang-distributed SEIR epidemic models with cross-diffusion. *Mathematics* **2023**, *11*, 2167. [CrossRef]
22. Sabbar, Y.; Khan, A.; Din, A.; Tilioua, M. New method to investigate the impact of independent quadratic α-stable Poisson jumps on the dynamics of a disease under vaccination strategy. *Fractal Fract.* **2023**, *7*, 226. [CrossRef]
23. Dhandapani, P.B.; Leiva, V.; Martin-Barreiro, C.; Rangasamy, M. On a novel dynamics of a SIVR model using a Laplace-Adomian decomposition based on a vaccination strategy. *Fractal Fract.* **2023**, *7*, 407. [CrossRef]
24. Dhandapani, P.B.; Thippan, J.; Martin-Barreiro, C.; Leiva, V.; Chesneau, C. Numerical solutions of a differential system considering a pure hybrid fuzzy neutral delay theory. *Electronics* **2022**, *11*, 1478. [CrossRef]
25. Moustafa, E.S.; Ahmed, A. The fractional SIRC model and influenza. *Math. Probl. Eng.* **2011**, *2011*, 480378.
26. Sha, H.; Sanyi, T.; Libinin, R. A discrete stochastic model for COVID-19 outbreak: Forecast and control. *Math. Biosci. Eng.* **2020**, *14*, 2792–2804.
27. Chintamani, P.; Ankush, B.; Vaibhav, R. Investigating the dynamics of COVID-19 pandemic in India under lockdown. *Chaos Solitons Fractals* **2020**, *138*, 109988.
28. Khan, M.A.; Atangana, A. Modeling the dynamics of novel coronavirus (2019-nCov) with fractional derivative. *Alex. Eng. J.* **2020**, *59*, 2379–2389. [CrossRef]
29. Yang, X.J. *General Fractional Derivatives: Theory, Methods and Applications*; CRC Press: Boca Raton, FL, USA, 2019.
30. Baleanu, D.; Jajarmi, A.; Sajjadi, S.S.; Mozyrska, D. A new fractional model and optimal control of tumour immune surveillance with non-singular derivative operator. *Chaos* **2019**, *29*, 083127. [CrossRef]
31. Khan, A.; Bai, X.; Ilyas, M.; Rauf, A.; Xie, W.; Yan, P.; Zhang, B. Design and application of an interval estimator for nonlinear discrete-time SEIR epidemic models. *Fractal Fract.* **2022**, *6*, 213. [CrossRef]
32. Alyobi, S.; Jan R. Qualitative and quantitative analysis of fractional dynamics of infectious diseases with control measures. *Fractal Fract.* **2023**, *7*, 400. [CrossRef]
33. Alkady, W.; ElBahnasy, K.; Leiva, V.; Gad, W. Classifying COVID-19 based on amino acids encoding with machine learning algorithms. *Chemom. Intell. Lab. Syst.* **2022**, *224*, 104535. [CrossRef] [PubMed]
34. Sardar, I.; Akbar, M.A.; Leiva, V.; Alsanad, A.; Mishra, P. Machine learning and automatic ARIMA/Prophet models-based forecasting of COVID-19: Methodology, evaluation, and case study in SAARC countries. *Stoch. Environ. Res. Risk Assess.* **2022**, *37*, 345–359. [CrossRef] [PubMed]
35. Liu, Y.; Mao, C.; Leiva, V.; Liu, S.; Silva Neto, W.A. Asymmetric autoregressive models: Statistical aspects and a financial application under COVID-19 pandemic. *J. Appl. Stat.* **2021**, *49*, 1323–1347. [CrossRef] [PubMed]
36. Mahdi, E.; Leiva, V.; Mara'Beh, S.; Martin-Barreiro, C. A new approach to predicting cryptocurrency returns based on the gold prices with support vector machines during the COVID-19 pandemic using sensor-related data. *Sensors* **2021**, *21*, 6319. [CrossRef]
37. Jerez-Lillo, N.; Lagos Alvarez, B.; Munoz Gutierrez, J.; Figueroa-Zuniga, J.; Leiva, V. A statistical analysis for the epidemiological surveillance of COVID-19 in Chile. *Signa Vitae* **2022**, *18*, 19–30.
38. Leiva, V.; Alcudia, E.; Montano, J.; Castro, C. An epidemiological analysis for assessing and evaluating COVID-19 based on data analytics in Latin American countries. *Biology* **2023**, *12*, 887. [CrossRef]
39. Martin-Barreiro, C.; Ramirez-Figueroa, J.A.; Cabezas, X.; Leiva, V.; Galindo-Villardón, M.P. Disjoint and functional principal component analysis for infected cases and deaths due to COVID-19 in South American countries with sensor-related data. *Sensors* **2021**, *21*, 4094. [CrossRef]

40. Cavalcante, T.; Ospina, R.; Leiva, V.; Cabezas, X.; Martin-Barreiro, C. Weibull regression and machine learning survival models: Methodology, comparison, and application to biomedical data related to cardiac surgery. *Biology* **2023**, *12*, 442. [CrossRef] [PubMed]
41. Kermack, W.O.; McKendrick, A.G. Contribution to the mathematical theory of epidemics. *Proc. R. Soc. Lond.* **1927**, *115*, 700–721.
42. Abishek, K.; Kanica, G.; Nilam. A deterministic time-delayed SIR epidemic model: Mathematical modelling and analysis. *Theory Biosci.* **2020**, *139*, 67–76.
43. Nisar, K.S.; Ahmad, S.; Ullah, A.; Shah, K.; Alrabaiah, H.; Arfan, M. Mathematical analysis of SIRD model of COVID-19 with Caputo fractional derivative based on real data. *Results Phys.* **2021**, *21*, 103772. [CrossRef] [PubMed]
44. Rodr, R.G.; Go, A.R. Generalized SIRD epidemiological model for COVID-19 in Tolima-Colombia. *J. Popul. Ther. Clin. Pharmacol.* **2023**, *30*, e1–e7.
45. Cihan, P. Fuzzy rule-based system for predicting daily case in COVID-19 outbreak. In Proceedings of the 4th International Symposium on Multidisciplinary Studies and Innovative Technologies, Istanbul, Turkey, 22–24 October 2020; pp. 1–4.
46. Kandel, A. *Fuzzy Mathematical Techniques with Applications*; Addison-Wesley: New York, NY, USA, 1986.
47. Caputo, M.; Fabrizio, M. A new definition of fractional derivative without singular kernel. *Prog. Fract. Differ. Appl.* **2015**, *1*, 73–85.
48. Scarf, H.E.; Shoven, J.B. *Applied General Equilibrium Analysis*; Cambridge Books: Cambridge, UK, 2008.
49. Qian, D.; Li, C.; Agarwal, R.P.; Wong, P.J.Y. Stability analysis of fractional differential system with Riemann-Liouville derivative. *Math. Comput. Model.* **2010**, *52*, 862–874. [CrossRef]
50. Basti, B.; Hammami, N.; Berrabah, I.; Nouioua, F.; Djemiat, R.; Benhamidouche, B. Stability analysis and existence of solutions for a modified SIRD model of COVID-19 with fractional derivatives. *Symmetry* **2021**, *13*, 1431. [CrossRef]